Enhancing permittivity of ferroelectric superlattices via composition tuning

N. A. Pertsev,[1,2] P.-E. Janolin,[2] J.-M. Kiat,[2,3] and Y. Uesu[4]
[1]*A. F. Ioffe Physico-Technical Institute, Russian Academy of Sciences, 194021 St. Petersburg, Russia*
[2]*Laboratoire Structures, Propriétés et Modélisation des Solides, UMR CNRS-École Centrale Paris, 92295 Châtenay-Malabry, France*
[3]*Laboratoire Léon Brillouin, CE Saclay CNRS-UMR 12, 91991 Gif-Sur-Yvette Cedex, France*
[4]*Department of Physics, Waseda University, 3-4-1 Okubo, Shinjuku-ku, Tokyo 169-8555, Japan*
(Received 16 January 2010; revised manuscript received 23 February 2010; published 19 April 2010)

A nonlinear thermodynamic theory is applied to strained ferroelectric superlattices and used to determine the dependence of superlattice permittivity on composition. To that end, spontaneous polarizations and field-induced polarization changes in the ferroelectric layers A and B with thicknesses t_A and t_B are calculated as a function of the volume fraction $\phi_A = t_A/(t_A+t_B)$. The existence of a dielectric anomaly at a specific composition ϕ_A^* is predicted for the superlattices, where only one of ferroelectric layers has nonzero out-of-plane polarization in the uncoupled state. The theoretical predictions agree with the composition dependence of permittivity displayed by the $Pb(Sc_{1/2}Nb_{1/2})O_3/PbTiO_3$ superlattices grown on $SrRuO_3$-covered $SrTiO_3$.

DOI: 10.1103/PhysRevB.81.144118 PACS number(s): 77.22.Ch, 77.55.fg, 77.55.Px, 77.80.B−

I. INTRODUCTION

Owing to their unique physical properties, ferroelectrics have many potential and already implemented applications in the microelectronics, with nonvolatile ferroelectric memories, actuators, sensors, and magnetoelectric devices being some representative examples.[1] However, the integration of ferroelectric components in microelectronic systems requires the use of thin films, which often have performances significantly degraded in comparison with bulk ferroelectrics. An efficient way to tackle this problem could be the replacement of homogeneous films by ferroelectric superlattices composed of two (or several) dissimilar materials. Indeed, the tuning of superlattice composition and period offers additional opportunities for enhancing the physical properties of thin-film ferroelectrics. This conjecture is supported by the successful fabrication of various ferroelectric superlattices[2–10] and the observation of polarization enhancement in the $SrTiO_3/BaTiO_3/CaTiO_3$ stack.[8] Moreover, superlattices may display unexpected properties which cannot be predicted from those of isolated constituent materials. For instance, $BaZrO_3/SrTiO_3$ and $SrZrO_3/SrTiO_3$ superlattices were found to be ferroelectric despite the fact that they are composed of paraelectric materials.[4,5]

The dielectric properties of ferroelectric superlattices were studied experimentally for several material combinations and a pronounced dependence of permittivity on period was revealed.[3] In some studies, a huge dielectric response was observed, which exceeds the permittivity of compositionally equivalent bulk solid solution by several orders of magnitude. However, these dielectric anomalies are not intrinsic; they should be attributed to the Maxwell-Wagner behavior resulting from the presence of low-resistivity interfacial regions in some superlattices, which separate normal ferroelectric layers.[11]

The composition dependence of superlattice dielectric response was not the subject of detailed experimental studies for some time. Only recently, it has been measured for the $PbSc_{1/2}Nb_{1/2}O_3/PbTiO_3$ (PSN/PT) superlattice.[12,13] This material system corresponds to the class of solid solutions exhibiting a morphotropic phase boundary (MPB), which attract considerable interest due to enhancement of many physical properties in a specific range of concentrations (see Ref. 14 and references therein). The dielectric measurements showed that the permittivity of PSN/PT superlattice varies nonmonotonically with composition, reaching maximum at an equivalent PT concentration $x \approx 32\%$.[13] Remarkably, this value differs considerably from the MPB concentration $x \approx 43\%$, at which the permittivity becomes maximal in bulk PSN/PT ceramics.[15,16] Hence the dielectric peak observed in ferroelectric superlattices may have another origin, which points to a strong need for the theoretical analysis of their dielectric properties.

Ferroelectric superlattices were investigated theoretically by several methods including the phenomenological approach[17–20] and the first-principles calculations.[21–24] The effects of interfacial coupling, electrostatic interactions and substrate-induced lattice strains on their physical properties were considered. The composition dependence of permittivity, however, was explicitly addressed only for superlattices with alternating ferroelectric and paraelectric layers.[18]

In this paper, we analyze the composition dependence of the polarization states and permittivity in superlattices composed of two different perovskite ferroelectrics. Numerical calculations are performed for a superlattice involving strained $Pb(Zr_{0.5}Ti_{0.5})O_3$ and $PbTiO_3$ layers. The theoretical results are compared with the experimental data available for the $Pb(Sc_{1/2}Nb_{1/2})O_3/PbTiO_3$ superlattices grown on $SrRuO_3$-covered $SrTiO_3$.

II. THERMODYNAMIC CALCULATIONS

We focus on periodic superlattices consisting of alternating layers of ferroelectrics A and B. The superlattice is assumed to be epitaxially grown on a bottom electrode deposited on a thick substrate and covered by a top electrode. Owing to the lattice matching at the interfaces and a different thermal expansion coefficient of the substrate, ferroelectric layers are generally strained to a certain extent. In the usual case of an isotropic biaxial strain imposed on the superlattice

by the electrode-substrate couple, the in-plane lattice strains in the slabs A and B are defined by the relations $u_{A11}=u_{A22}=(a_A-a_{A0})/a_{A0}$, $u_{B11}=u_{B22}=(a_B-a_{B0})/a_{B0}$, and $u_{A12}=u_{B12}=0$. Here a_A and a_B are the in-plane lattice parameters in the strained layers A and B, whereas a_{A0} and a_{B0} are the lattice constants of the free-standing layers in the prototypic cubic phase, which is assumed to have the (001) orientation with respect to the interfaces. It should be emphasized that in the coherent superlattices ($a_A=a_B$) ferroelectric layers are generally strained to a different extent because of unequal lattice constants a_{A0} and a_{B0}.

It is known that lattice strains have a strong impact on the polarization state of an epitaxial ferroelectric film.[25,26] In films of perovskite ferroelectrics such as $BaTiO_3$, $PbTiO_3$, and $Pb(Zr_{1-x}Ti_x)O_3$ (PZT), the orientation of the spontaneous polarization $\mathbf{P}_s$ changes from the out-of-plane direction at large compressive strains $u_{11}=u_{22}=u_m<0$ to the in-plane one at large tensile strains $u_m>0$. Since the stability ranges of different polarization states vary from one ferroelectric material to another, in some ferroelectric superlattices the strain effect favors different polarization orientations in the layers A and B. At the same time, the electrostatic coupling between these layers tends to eliminate the mismatch between the out-of-plane polarization components P_{A3} and P_{B3}, which creates an internal electric field in the superlattice. The interplay of the strain and electrostatic effects may result, as will be shown below, in a strong enhancement of the superlattice dielectric response at a certain composition.

For the theoretical description of this interplay, it is sufficient to employ the approximation of uniformly polarized and homogeneously strained layers. Accordingly, we shall consider only relatively thick layers with thicknesses $t_A \gg a_{A0}$ and $t_B \gg a_{B0}$, where the microscopic effects caused by local interfacial coupling[17,24] may be neglected. Then the mean Helmholtz free-energy density $\langle F\rangle$ of the A/B superlattice can be written as $\langle F\rangle=\phi_A F_A+(1-\phi_A)F_B$, where $\phi_A=t_A/(t_A+t_B)$ is the volume fraction of the ferroelectric A in the superlattice, and F_A and F_B are the energy densities in the layers A and B. For the Helmholtz free energy densities F_α ($\alpha=A$, B), the thermodynamic theory of ferroelectric films gives

$$F_\alpha = a^*_{\alpha 1}(P^2_{\alpha 1}+P^2_{\alpha 2})+a^*_{\alpha 3}P^2_{\alpha 3}+a^*_{\alpha 11}(P^4_{\alpha 1}+P^4_{\alpha 2})+a^*_{\alpha 33}P^4_{\alpha 3} + a^*_{\alpha 12}P^2_{\alpha 1}P^2_{\alpha 2}+a^*_{\alpha 13}(P^2_{\alpha 1}+P^2_{\alpha 2})P^2_{\alpha 3}+\ \ldots-\frac{1}{2}\varepsilon_0 E^2_{\alpha 3} - P_{\alpha 3}E_{\alpha 3}, \quad (1)$$

where $a^*_{\alpha j}$ and $a^*_{\alpha jk}$ ($j,k=1,2,3$) are the renormalized coefficients of the second- and fourth-order polarization terms given in Ref. 27. For brevity, we omitted in Eq. (1) the higher-order polarization terms, which do not depend of the mechanical boundary conditions, as well as the terms independent of polarization. The electric fields $\mathbf{E}_A$ and $\mathbf{E}_B$ existing inside the layers A and B were assumed to be orthogonal to the interfaces. The out-of-plane field components E_{A3} and E_{B3} satisfy the relation $\phi_A E_{A3}+(1-\phi_A)E_{B3}=E$, where E is the mean electric field in the superlattice governed by the difference between electrostatic potentials of electrodes and their work functions. Since the electric displacement $\mathbf{D}=\varepsilon_0\,\mathbf{E}+\mathbf{P}$ should remain constant across the superlattice, we have $E_{A3}=E-(1-\phi_A)(P_{A3}-P_{B3})/\varepsilon_0$ and $E_{B3}=E+\phi_A(P_{A3}-P_{B3})/\varepsilon_0$, where ε_0 is the permittivity of vacuum. The substitution of these formulas into Eq. (1) makes the energy densities F_A and F_B interrelated at $P_{A3}\neq 0$ and/or $P_{B3}\neq 0$. As a result, the electrostatic coupling between the out-of-plane polarizations P_{A3} and P_{B3} becomes explicitly included in the mean free energy density $\langle F\rangle$.

The superlattice polarization state at a given temperature T, volume fraction ϕ_A, misfit strains u_{Am} and u_{Bm}, and electric field E can be determined via the minimization of the mean energy density $\langle F\rangle$. In general, it is a function of six variables, $P_{\alpha j}$, but the symmetry considerations make it possible to reduce the number of independent variables. In particular, when the orthorhombic aa phase ($|P_1|=|P_2|\neq 0$, $P_3=0$) or the monoclinic r phase ($|P_1|=|P_2|\neq 0$, $P_3\neq 0$) forms in a strained ferroelectric layer,[25,26] the two in-plane polarization components may be set equal to each other.

The small-signal out-of-plane permittivity ε_{33} of a ferroelectric superlattice can be calculated from the formula $\varepsilon_{33}=\varepsilon_0+[\phi_A\Delta P_{A3}+(1-\phi_A)\Delta P_{B3}]/\Delta E$, where ΔP_{A3} and ΔP_{B3} are the polarization changes induced in the layers A and B by a weak measuring field $\Delta E\to 0$. To find the quantities $\Delta P_{\alpha 3}\sim\Delta E$, one has to determine the electric field changes ΔE_{A3} and ΔE_{B3} inside the slabs A and B and, in general, the changes $\Delta P_{\alpha 1}$ and $\Delta P_{\alpha 2}$ of in-plane polarization components as well. The unknowns $\Delta P_{\alpha j}$ and $\Delta E_{\alpha 3}$ can be calculated using the equations of state $E_{\alpha j}=-\partial F_\alpha/\partial P_{\alpha j}$ linearized with respect to small quantities $\Delta P_{\alpha j}$ and the equalities $\Delta E_{A3}+\Delta P_{A3}/\varepsilon_0=\Delta E_{B3}+\Delta P_{B3}/\varepsilon_0$ and $\phi_A\Delta E_{A3}+(1-\phi_A)\Delta E_{B3}=\Delta E$ following from the electrostatic conditions. This approach leads to a system of eight linear equations with eight unknowns, which reduces to a system of six equations in the case of $\Delta P_{\alpha 1}=\Delta P_{\alpha 2}$.

For the numerical calculations, we selected the $Pb(Zr_{0.5}Ti_{0.5})O_3/PbTiO_3$ (PZT/PT) superlattice as a representative material system. The thermodynamic coefficients, elastic stiffnesses, and electrostrictive constants of the involved ferroelectrics are known[28] so that Eq. (1) can be used for quantitative predictions. The polarization states of PZT and PT layers at room temperature and the superlattice dielectric response were calculated as a function of composition. Several different values were taken for the misfit strains u_{PZT} and u_{PT} in order to model superlattices with different combinations of polarization orientations in two ferroelectric layers.

We first performed the calculations for ferroelectric superlattices sandwiched between identical top and bottom electrodes. Since there is no difference in the electrode work functions in this case, the mean electric field E equals zero in a short-circuited capacitor. Figure 1 shows variations of polarization components in the PZT and PT layers as a function of the volume fraction ϕ_{PT} of PT in the superlattice. Let us discuss first the results obtained for the superlattice, where the PZT layers are at a compressive misfit strain $u_{PZT}=-1\%$, whereas the PT ones are subjected to a tensile strain $u_{PT}=+2\%$. In this situation, the strain effect favors the out-of-plane polarization state in PZT layers and the in-plane

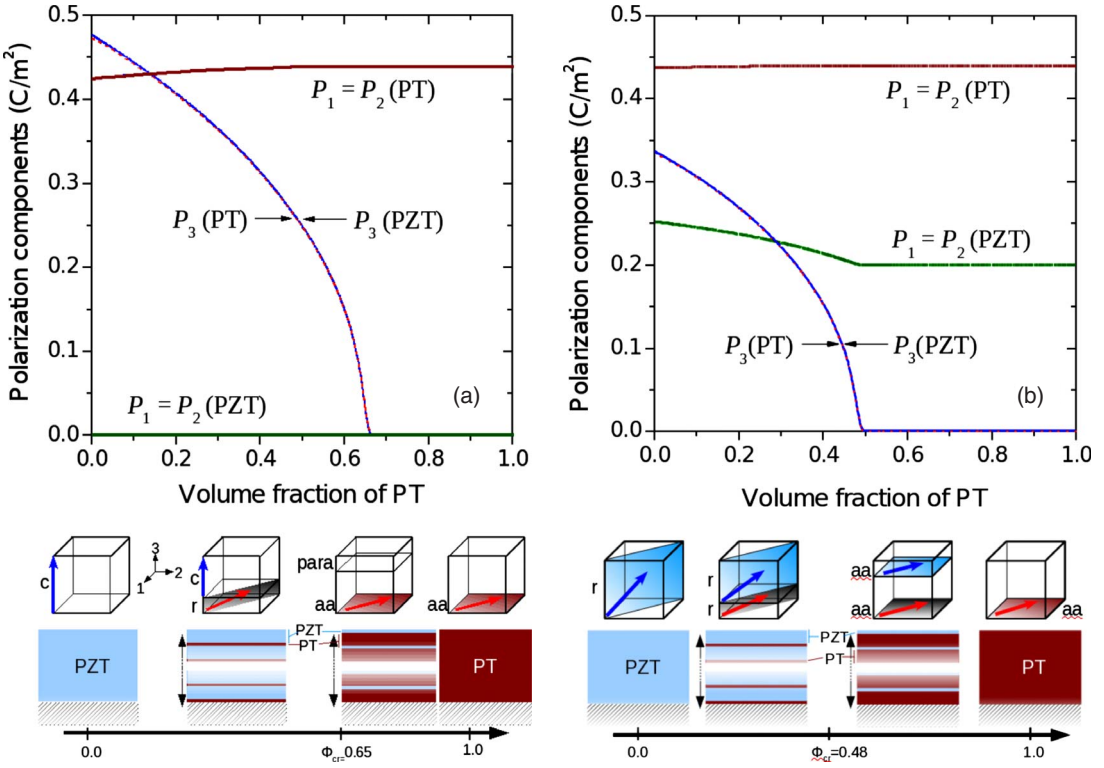

FIG. 1. (Color online) Polarization components in the strained $Pb(Zr_{0.5}Ti_{0.5})O_3/PbTiO_3$ superlattice as a function of composition at room temperature. The $PbTiO_3$ layers are subjected to a tensile biaxial in-plane strain of +2%, while the $Pb(Zr_{0.5}Ti_{0.5})O_3$ layers are under a compressive strain of −1% (a) or −0.2% (b).

polarization in the PT ones.[25,26] As is seen from Fig. 1(a), these states indeed appear in the superlattice at sufficiently large volume fractions of PZT and PT, respectively. Owing to the electrostatic coupling between two contacting ferroelectrics, however, other polarization states can form in the strained PZT and PT layers as well. Specifically, an out-of-plane polarization becomes induced in the PT slabs at $\phi_{PT} \leq 0.65$, which results in the formation of the *r* phase with the polarization inclined to the interfaces. In this range of ϕ_{PT}, there is only a very small difference between the polarization components P_{A3} and P_{B3}, which decrease with increasing volume fraction of PT. At $\phi_{PT} > 0.65$, the out-of-plane polarization disappears in the whole superlattice because it is energetically unfavorable in PT at a tensile strain of 2%. Thus, a phase transition takes place in the superlattice at $\phi_{PT}^* \cong 0.65$, being driven by the electrostatic interaction between two dissimilar ferroelectrics. This transition has the same origin as the suppression of ferroelectricity predicted by Roytburd *et al.* for the ferroelectric-paraelectric bilayers.[18] In our case, however, the superlattice retains ferroelectricity at both subcritical and overcritical compositions. For the PT volume fractions above ϕ_{PT}^*, it is energetically favorable to combine the ferroelectric in-plane polarization state (*aa* phase) in the PT layers with the paraelectric PZT slabs, whereas at $\phi_{PT} < \phi_{PT}^*$ the out-of-plane polarization state (*c* phase) in PZT layers coexists with the ferroelectric *r* phase in the PT ones.

A phase transition at some critical volume fraction ϕ_{PT}^* also occurs when the strain effect favors the *r* phase in PZT layers and the in-plane polarization state in PT slabs. Figure 1(b) shows the results obtained for a representative superlattice, where the misfit strain imposed on PZT layers has been changed to $u_{PZT} = -0.2\%$ in order to stabilize the monoclinic *r* state at $\phi_{PZT} \to 1$.[26] It can be seen that at $\phi_{PT} < \phi_{PT}^* \cong 0.484$ the polarization in both ferroelectrics is inclined to the interfaces, but with different inclination angles. The out-of-plane component is almost the same in the PZT and PT layers; it gradually reduces with increasing ϕ_{PT} and reaches zero at ϕ_{PT}^*. This results in the transformation of the *r* phase into the in-plane polarization state in both layers. The polarization magnitude becomes independent of ϕ_{PT}, being about two times larger in the PT layers ($P_{A1} \cong 0.2$ C/m^2 vs. $P_{B1} \cong 0.44$ C/m^2). It should be noted that, at $\phi_{PT} < \phi_{PT}^*$, the in-plane polarization component in PZT slabs decreases with the reduction in the out-of-plane one. This unexpected behavior, which contrasts with the polarization rotation under varying misfit strain,[26] is due to the fact that the coefficient a_{A13}^* of the relevant coupling term $a_{A13}^*(P_{A1}^2 + P_{A2}^2)P_{A3}^2$ in Eq. (1) is negative for PZT.

Since at both phase transitions described above the out-of-plane polarization tends to zero at $\phi_{PT} \to \phi_{PT}^*$, the superlattice permittivity ε_{33} should increase drastically near the critical composition ϕ_{PT}^*. Figure 2(a) illustrates the dependence of ε_{33} on the volume fraction of PT in the superlattice. As we assumed the polarization to be uniform within each ferroelectric layer, the permittivity diverges at $\phi_{PT} = \phi_{PT}^*$ for both studied superlattices. This divergence of course cannot appear in real superlattices because of polarization inhomogeneities caused by the presence of defects and 180° domains.

The results presented in Fig. 2(a) indicate that the critical composition of the A/B superlattice depends on the misfit strains u_{Am} and u_{Bm} imposed on the A and B layers. Since the polarization components P_{A3} and P_{B3} go to zero at $\phi_A \to \phi_A^*$, an approximate analytical formula can be derived for the dependence $\phi_A^*(u_{Am}, u_{Bm})$. Setting $P_{A3}=P_{B3}=P_3$ and neglecting in Eq. (1) the sixth-order terms in P_{A3} and P_{B3}, from the condition $P_3(\phi_A)=0$ we obtain

$$\phi_A^* \approx \frac{a_{B3}^* + 2a_{B13}^* P_{B1}^2 + (2a_{B112} + a_{B123})P_{B1}^4}{a_{B3}^* + 2a_{B13}^* P_{B1}^2 + (2a_{B112} + a_{B123})P_{B1}^4 - a_{A3}^* - 2a_{A13}^* P_{A1}^2 - (2a_{A112} + a_{A123})P_{A1}^4}, \tag{2}$$

where the in-plane polarization components $P_{A1}=P_{A2}$ and $P_{B1}=P_{B2}$ should be calculated from the equations $\partial F_\alpha / \partial P_{\alpha 1}=0$ with $P_{\alpha 3}$ set to zero. Equation (2) demonstrates that the dependence of ϕ_A^* on the misfit strains is governed by linear variations of the renormalized thermodynamic coefficients $a_{A3}^*(u_{Am})$ and $a_{B3}^*(u_{Bm})$ combined with nonlinear changes of P_{A1} and P_{B1} resulting from linear variations of the coefficients $a_{A1}^*(u_{Am})$ and $a_{B1}^*(u_{Bm})$. For the superlattices without in-plane polarization components, Eq. (2) reduces to $\phi_A^* \approx a_{B3}^*/(a_{B3}^* - a_{A3}^*)$. We see that the critical volume fraction $0<\phi_A^*<1$ does not exist when both layers stabilize in the ferroelectric c phase ($a_{A3}^*<0$ and $a_{B3}^*<0$), but appears in superlattices, where the c phase coexists with the paraelectric one ($a_{A3}^*<0$ and $a_{B3}^*>0$ or vice versa).

When the superlattice is sandwiched between dissimilar electrodes, as in many experimental studies,[10,12,13] the mean internal electric field E becomes different from zero even in the short-circuited capacitor. In particular, the difference ΔW in electrode work functions gives rise to the field $E=\Delta W/t$, where t is the distance between electrodes.[29] This field smears the dielectric anomaly at $\phi_{PT}=\phi_{PT}^*$, as shown in Fig. 2(b) for the typical combination of an elemental metal electrode and a conductive oxide one (we take $\Delta W=0.2$ eV as in the case of Au and $SrRuO_3$ electrodes[30]). A similar smearing effect may appear in superlattices with differing AB and BA interfaces[24] and in capacitors with dissimilar top and bottom ferroelectric-electrode interfaces.[31]

It should be noted that the internal electric field E makes the out-of-plane polarizations P_{A3} and P_{B3} different from zero in the whole range $0<\phi_A<1$ because a constant term $-E$ appears in the equations $\partial F_\alpha / \partial P_{\alpha 3}=0$ defining these components. As a result, the superlattice permittivity $\varepsilon_{33}(\phi_A)$ becomes finite for all compositions, and the exact position of the dielectric peak shifts from the critical volume fraction ϕ_A^* given by Eq. (2). Figure 2(b) demonstrates that, in the studied PZT/PT superlattices, this peak appears at a *higher* PT volume fraction ϕ_{PT}^{max}, with the shift $\Delta\phi_{PT}=\phi_{PT}^{max}-\phi_{PT}^*$ being larger for a stronger internal field E.

III. COMPARISON WITH EXPERIMENT

As there are no dielectric measurements performed for PZT/PT superlattices, we have used the experimental data[12,13] obtained for $Pb(Sc_{1/2}Nb_{1/2})O_3/PbTiO_3$ (PSN/PT) superlattices grown on $SrRuO_3$-covered $SrTiO_3$ in order to make a qualitative comparison with our theoretical results.

From the reported lattice parameters, the misfit strain has been evaluated to be almost zero in PSN layers and about +2% in PT ones for all the compositions investigated. Therefore, the PT layers in accordance with the thermodynamic theory of ferroelectric films[25] should adopt the *aa* polarization state, whereas the PSN layers are in a monoclinic phase according to the recent first-principles-based calculations.[32] It should be noted that a complete analysis of the strain state existing in PSN films deposited on $SrTiO_3$ points to the tetragonal symmetry,[33] but there are experimental proofs that small monoclinic distortions do exist here.[34] Moreover, one has to take into account that lattice strains in a superlattice may be quite different from those in a homogeneous film, as, for instance, the slabs of PSN are deposited on strained PT instead of $SrTiO_3$.

The polarization state in PSN/PT superlattices is therefore analogous to the one shown in Fig. 1(b), with PSN replacing PZT. The evolution of the out-of-plane permittivity ε_{33} with composition, which was measured for the PSN/PT superlattice films with the constant total thickness of 100 nm,[13] is shown in Fig. 3. It is seen that the permittivity exhibits a maximum at the PT volume fraction $\phi_{PT}^* \approx 0.32$. Remarkably, the shape of the observed dependence $\varepsilon_{33}(\phi_{PT})$ is similar to the theoretical curve 3 in Fig. 2(b), which is distinguished by a maximum at $\phi_{PT}^* \cong 0.34$ and the relation $\varepsilon_{33}(\phi_{PT}=0) > \varepsilon_{33}(\phi_{PT}=1)$. Thus, the dielectric peak displayed by the PSN/PT superlattices can be attributed to the suppression of the out-of-plane component of the spontaneous polarization in PSN layers, which is caused by the presence of strained PT layers tending to stabilize in an in-plane polarization state.

We would like to emphasize that the proposed enhancement mechanism is fundamentally different from those operating at the morphotropic phase boundary (MPB) in bulk ferroelectric solid solutions and in monoclinic thin films. Haumont *et al.*[15] have reported an enhancement of the dielectric response at the MPB existing in the phase diagram of bulk PSN-PT (see Fig. 1 in Ref. 15). However, in the case of bulk compounds the origin of this enhancement is explained on the basis of competition between two ground states of the end members, where the spontaneous polarization has different fixed directions, pointing along the [111] axis in bulk PSN and along the [100] axis in bulk PT. This competition induces the stabilization of monoclinic phases, as demonstrates by *ab initio* calculations.[15,16] In these monoclinic

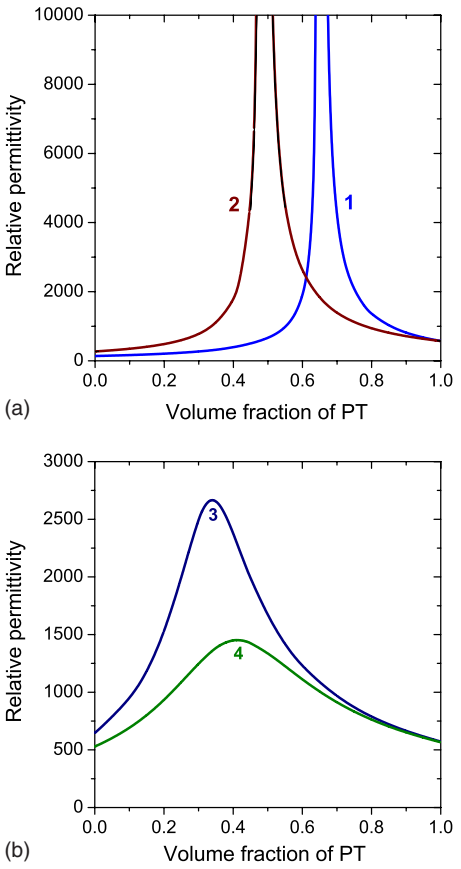

FIG. 2. (Color online) Relative out-of-plane permittivity $\varepsilon_{33}/\varepsilon_0$ of the strained $Pb(Zr_{0.5}Ti_{0.5})O_3/PbTiO_3$ superlattice as a function of composition at room temperature. Panel (a) shows the dependences calculated for two differently strained superlattices sandwiched between identical electrodes. Here u_{PT}=+2%, whereas u_{PZT}=−1% (curve 1) or u_{PZT}=−0.2% (curve 2). Panel (b) demonstrates the dielectric response of the superlattice with dissimilar top and bottom electrodes. Here the total thickness of ferroelectric layers with strains u_{PZT}=+0.4% and u_{PT}=+2% is taken to be 100 nm (curve 3) or 40 nm (curve 4), while the difference in the electrode work functions amounts to 0.2 eV.

phases, polarization is no more constrained to a particular crystallographic direction, but can rotate freely inside the monoclinic plane, making the response to an external action (electric field, stress, pressure, temperature, etc.) very large. A similar mechanism is responsible for the enhanced properties of thin films adopting a monoclinic symmetry, operating, for example, in the PSN-43%PT thin film deposited on $SrTiO_3$.[34] One has to note, however, that in the case of thin films it is the misfit strain that causes the properties to be enhanced, and that the composition is of lesser importance than in the bulk compounds (see Ref. 35). In the case of superlattices, a third mechanism emerges: the electrostatic coupling between the out-of-plane polarization components in dissimilar ferroelectric layers.

IV. CONCLUDING REMARKS

In this work, the polarization states and out-of-plane permittivity of PZT/PT superlattices were calculated with the aid of the nonlinear thermodynamic theory of strained ferroelectric films. It was found that the composition dependence of superlattice permittivity is governed by the polarization states of ferroelectric layers, which would appear in the absence of their electrostatic coupling. Namely, when the out-of-plane polarization is present (or absent) in both uncoupled ferroelectric layers, the permittivity varies with composition monotonically. In contrast, a dielectric anomaly appears at a certain critical composition in the case of superlattices, where this polarization exists in one of uncoupled ferroelectric layers only.

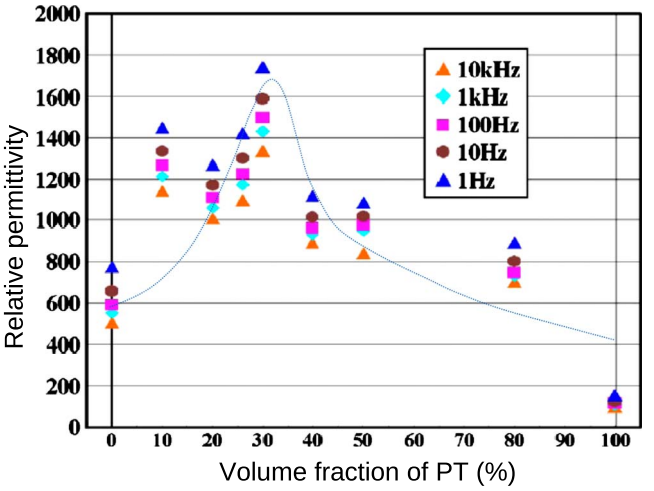

FIG. 3. (Color online) Variation in the relative permittivity with composition in the $Pb(Sc_{1/2}Nb_{1/2})O_3/PbTiO_3$ superlattices measured at different frequencies indicated on the plot (adapted from Ref. 13). The blue line is a guide for the eyes.

Importantly, the critical composition is sensitive to the strain states of constituent materials and to the magnitude of internal electric field in the capacitor (see Fig. 2). For instance, the critical volume fraction of PT in the PZT/PT superlattice decreases with increasing misfit strain u_{PZT} in PZT layers, shifting from $\phi^*_{PT} \cong 0.65$ to about 0.48 when u_{PZT} changes from −1% to −0.2%, as demonstrated by Fig. 2(a). On the contrary, the dielectric anomaly migrates to a higher PT volume fraction with the increase of internal electric field in the capacitor [see Fig. 2(b)]. Our theoretical calculations reproduce the PT volume fraction $\phi^*_{PT} \approx 0.3$, at which the maximum permittivity is observed in PSN/PT superlattices. Although the thermodynamic parameters of PSN differ from those of PZT, this difference may be compensated by the strain effect since the misfit strains are not the same in the PSN/PT and PZT/PT superlattices. The first-principles-based calculations of ferroelectric states in bulk PSN crystals[32] open the possibility for accurate theoretical description of strained PSN/PT superlattices in the future.

Since the physical origin of the discussed dielectric anomaly is very general, our theoretical prediction of two qualitatively different composition dependences of permittivity is valid for various ferroelectric superlattices with many combinations of polarization "ground" states. For superlattices of perovskite ferroelectrics fabricated on cubic, tetragonal, and orthorhombic substrates, the most important combinations providing a dielectric peak involve the *c* phase, *r*

phase, or *ac* phase ($P_1 \neq 0$, $P_2=0$, $P_3 \neq 0$) in one of uncoupled layers and the *aa* phase or *a* phase ($P_1 \neq 0$, $P_2=0$, $P_3=0$) in the other. Indeed, the composition dependence remains qualitatively the same within the stability ranges of polarization ground states in the misfit strain-temperature plane, but the critical composition varies with strain and temperature.

Finally, we note that, in the case of single-domain ferroelectric layers considered in this paper, there is no dependence of permittivity on the superlattice period. This behavior holds, however, only for coherent superlattices not containing misfit dislocations at the interfaces between ferroelectric slabs. The generation of misfit dislocations at larger layer thicknesses and an increase in their density with increasing period should result in significant changes of superlattice permittivity. (These dislocations will also modify the dependence of permittivity on composition at a fixed period. However, they should not suppress the appearance of predicted dielectric anomaly in appropriate incoherent superlattices despite variations of misfit strains with layer thicknesses in this case.) On the other hand, when the period decreases down to the nanoscale range, the short-range interfacial effects come into play. As a result, the permittivity of short-period superlattices should begin to vary with period as well. The influence of short-range coupling on the superlattice permittivity can be modeled by the introduction of interfacial nanolayers with a permittivity different from those of both constituents.[36]

[1] J. F. Scott, Science **315**, 954 (2007).
[2] K. Iijima, T. Terashima, Y. Bando, K. Kamigaki, and H. Terauchi, J. Appl. Phys. **72**, 2840 (1992).
[3] H. Tabata, H. Tanaka, and T. Kawai, Appl. Phys. Lett. **65**, 1970 (1994).
[4] H. M. Christen, E. D. Specht, S. S. Silliman, and K. S. Harshavardhan, Phys. Rev. B **68**, 020101(R) (2003).
[5] T. Tsurumi, T. Harigai, D. Tanaka, S. M. Nam, H. Kakemoto, S. Wada, and K. Saito, Appl. Phys. Lett. **85**, 5016 (2004).
[6] Y. Lu, Appl. Phys. Lett. **85**, 979 (2004).
[7] M. Dawber, C. Lichtensteiger, M. Cantoni, M. Veithen, P. Ghosez, K. Johnston, K. M. Rabe, and J.-M. Triscone, Phys. Rev. Lett. **95**, 177601 (2005).
[8] H. N. Lee, H. M. Christen, M. F. Chisholm, C. M. Rouleau, and D. H. Lowndes, Nature (London) **433**, 395 (2005).
[9] H. Bouyanfif, M. El Marssi, N. Lemée, F. Le Marrec, M. G. Karkut, and B. Dkhil, Phys. Rev. B **71**, 020103(R) (2005).
[10] M. Tyunina, I. Jaakola, J. Levoska, and M. Plekh, Phys. Rev. B **76**, 134107 (2007).
[11] G. Catalan, D. O'Neill, R. M. Bowman, and J. M. Gregg, Appl. Phys. Lett. **77**, 3078 (2000).
[12] S. Asanuma, Y. Uesu, C. Malibert, and J.-M. Kiat, Appl. Phys. Lett. **90**, 242910 (2007).
[13] S. Asanuma, Y. Uesu, C. Malibert, and J.-M. Kiat, J. Appl. Phys. **103**, 094106 (2008).
[14] J.-M. Kiat and B. Dkhil, in *Handbook of Advanced Dielectric, Piezoelectric and Ferroelectric Materials: Synthesis, Properties and Applications*, edited by Z.-G. Ye (Woodhead Publishing Limited, Cambridge, 2008), p. 391.
[15] R. Haumont, B. Dkhil, J.-M. Kiat, A. Al-Barakaty, H. Dammak, and L. Bellaiche, Phys. Rev. B **68**, 014114 (2003).
[16] R. Haumont, A. Al-Barakaty, B. Dkhil, J.-M. Kiat, and L. Bellaiche, Phys. Rev. B **71**, 104106 (2005).
[17] B. D. Qu, W. L. Zhong, and R. H. Prince, Phys. Rev. B **55**, 11218 (1997).
[18] A. L. Roytburd, S. Zhong, and S. P. Alpay, Appl. Phys. Lett. **87**, 092902 (2005).
[19] V. A. Stephanovich, I. A. Luk'yanchuk, and M. G. Karkut, Phys. Rev. Lett. **94**, 047601 (2005).
[20] F. A. Urtiev, V. G. Kukhar, and N. A. Pertsev, Appl. Phys. Lett. **90**, 252910 (2007).
[21] J. B. Neaton and K. M. Rabe, Appl. Phys. Lett. **82**, 1586 (2003).
[22] I. A. Kornev and L. Bellaiche, Phys. Rev. Lett. **91**, 116103 (2003).
[23] E. Bousquet, M. Dawber, N. Stucki, C. Lichtensteiger, P. Hermet, S. Gariglio, J.-M. Triscone, and P. Ghosez, Nature (London) **452**, 732 (2008).
[24] X. Wu, M. Stengel, K. M. Rabe, and D. Vanderbilt, Phys. Rev. Lett. **101**, 087601 (2008).
[25] N. A. Pertsev, A. G. Zembilgotov, and A. K. Tagantsev, Phys. Rev. Lett. **80**, 1988 (1998).
[26] N. A. Pertsev, V. G. Kukhar, H. Kohlstedt, and R. Waser, Phys. Rev. B **67**, 054107 (2003).
[27] N. A. Pertsev, A. K. Tagantsev, and N. Setter, Phys. Rev. B **61**, R825 (2000).
[28] The sets of material parameters used in numerical calculations are (in SI units, temperature T in °C): dielectric stiffness coefficients at constant strain $a_1=1.33(T-392.6)\times10^5$, $a_{11}=5.26\times10^8$, $a_{12}=-1.847\times10^8$, $a_{111}=1.336\times10^8$, $a_{112}=6.128\times10^8$, and $a_{123}=-2.894\times10^9$ for $Pb(Zr_{0.5}Ti_{0.5})O_3$ and $a_1=3.8(T-479)\times10^5$, $a_{11}=4.229\times10^8$, $a_{12}=7.354\times10^8$, $a_{111}=2.6\times10^8$, $a_{112}=6.1\times10^8$, and $a_{123}=-3.7\times10^9$ for $PbTiO_3$; elastic stiffnesses at constant polarization $c_{11}=1.545\times10^{11}$, $c_{12}=8.405\times10^{10}$, and $c_{44}=3.484\times10^{10}$ for PZT and $c_{11}=1.746\times10^{11}$, $c_{12}=7.9365\times10^{10}$, and $c_{44}=1.11\times10^{11}$ for PT; electrostrictive constants in polarization notation $q_{11}=7.189\times10^9$, $q_{12}=-2.853\times10^9$, and $q_{44}=2.854\times10^9$ for PZT and $q_{11}=1.141\times10^{10}$, $q_{12}=4.603\times10^8$, and $q_{44}=7.5\times10^9$ for PT.
[29] J. G. Simmons, Phys. Rev. Lett. **10**, 10 (1963).
[30] A. J. Hartmann, M. Neilson, R. N. Lamb, K. Watanabe, and J. F. Scott, Appl. Phys. A: Mater. Sci. Process. **70**, 239 (2000).
[31] A. M. Bratkovsky and A. P. Levanyuk, Phys. Rev. Lett. **94**, 107601 (2005).
[32] P.-E. Janolin and L. Bellaiche (unpublished).
[33] P.-E. Janolin, J.-M. Kiat, C. Malibert, S. Asanuma, and Y. Uesu, Appl. Phys. Lett. **92**, 052908 (2008).
[34] R. Haumont, C. Malibert, B. Dkhil, J.-M. Kiat, F. LeMarrec, S. Asanuma, and Y. Uesu, Jpn. J. Appl. Phys. **45**, L42 (2006).
[35] P.-E. Janolin, J. Mater. Sci. **44**, 5025 (2009).
[36] N. A. Pertsev (unpublished).